A Synthetic Route toward Well-Defined Stoichiometric Silica Fullerene and Nanotubes Based on Metastable Four-Membered Rings

Dongju Zhang,*,†,‡ R. Q. Zhang,*,‡ Zhe Han,† and Chengbu Liu†

School of Chemistry and Chemical Engineering, Shandong University, Jinan, Shandong 250100, and Center of Super-Diamond and Advanced Films (COSDAF) and Department of Physics and Materials Science, City University of Hong Kong, Hong Kong SAR, China

Received: November 12, 2005; In Final Form: March 12, 2006

On the basis of computational considerations, using metastable four-membered rings as building blocks, we propose novel synthetic routes toward well-defined stoichiometric silica nanofullerenes and nanotubes. The viability of the routes has been demonstrated by performing high-level density functional calculations, and the so-formed nanoarchitectures were proved to be energetically and structurally stable. Such nanostructures, if synthesized, are expected to have potential application in nanotechnology.

1. Introduction

Great effort has been placed on synthesizing various nanoscale materials and researching their structure/property relationships since C_{60} fullerene[1] and carbon nanotubes[2] were discovered. As a particularly important molecular building material, silica has attracted considerable attention due to its technological importance in manufacturing semiconductors, catalysis, and many other scientific and industrial processes. Recently, considerable progress has been made in controllably fabricating individual silica structures into nanometer dimensions, including nanoclusters,[3,4] nanowires,[5,6] nanotubes,[7,8] nanospheres,[9,10] ultrathin films,[11] and mesoporous silicas.[12] However, challenges to the application of silica nanomaterials arise not only from making them but also from manipulating them to form devices. It is advantageous if one can directly produce desired nanostructures with unique properties for device fabrication. Such a technique has been feasible in producing silica nanoarchitectures ranging in size from only a few SiO_2 units to a few nanometers in diameter.[13,14]

A remarkable property of bulk silica is that it can form a number of different polymorphs, in which the local atomic coordinations are similar but the global networks formed are different. The structural diversity is even more complex for nanosized silica than for the bulk one, which provides materials with designed structures and properties. Many early and recent studies[15−31] have explored the structures and properties of various tailored nanoarchitectures of silica, including nanochains,[15−17,24,29,31] nanorings,[17−19,22,25,27,30] nanotubes,[21,23] nanocage-like structures,[26] and nanocages,[21,22,30] by performing quantum chemistry calculations. Our recent researches on this area focuses on enriching the database of silica nanostructures and understanding the forming mechanisms of silica nanomaterials. Our thin silica nanowires[29,31] were found to be energetically more favorable, thermally more stable, and chemically more reactive at the tip than the thinnest of those proposed earlier based on rhombic two-membered ring (2MR) molecular chains,[15−17,24] and were considered as appropriate structural models of one-dimensional (1D) silica nanowires. In contrast with chained silica models with nonbridging oxygen (NBO) defects on the ends of the chains, our 2MR−3MR hybrid models[30] can form stoichometric fully coordinated (i.e., desired 4- and 2-fold coordination for silicon and oxygen atoms, respectively) silica cages with relatively higher stabilities compared to early 2MR-based fully coordinated rings,[17] indicating the possibility to fabricate new extended silica polymorphs using 2MRs and 3MRs as building blocks. Another structural model of silica, based on pure 3MRs,[27] revealed a geometrically distinct type of silica clusters: highly symmetrical cage-like structures with good extendability to three-dimensional networks, which possess unique external channels and an internal cavity, and can be expected to act as potential precursors to form new silica polymorphs. These early and recent studies[15,16,32−34] of silica nanostructures have provided, on the atomic and molecular levels, useful information and fundamental understanding of the complicated nanostructures of silica. The following conclusions have been drawn: (i) the 2MR chains are the ground-state structures for the smallest silica clusters, $(SiO_2)_n$, with $n \leq 5$ (n denotes the number of SiO_2 units in a silica cluster),[30,31] (ii) the growth motif of the clusters changes at $n = 6$ into a more compact form composed of 3MRs,[31] (iii) the atomically well ordered fully coordinated structures, including ringed, caged, and tubular shapes, become energetically preponderant configurations for even longer silica clusters, i.e., $n \geq 18$.[21] Compared to the clusters with terminating defects, the fully coordinated silica nanostructures have been paid much greater attention because of their energetic and structural stabilities.[18,20,21,30] It is believed that there is a possibility of the realization of these energetically very favorable structures.[21] Further, these fully coordinated clusters have been used as models for researching the properties of various silica materials. For instance, de Leeuw et al.[23] reported the hydrolysis reactivity and stability of silica nanostructures by modeling the reaction of a fully coordinated 6MR-based nanotube with water, and Bromley et al.[18] studied vibrational models on a bulk silica surface using 2MR-based fully coordinated clusters. In view of the incredible diversity of silica nanostructures, we believe that these earlier proposed nanoarchitectures are still far to form the complete database.

* To whom correspondence should be addressed. E-mail: zhangdj@sdu.edu.cn (D.Z.); aprqz@cityu.edu.hk (R.Q.Z.).

† Shandong University.

‡ City University of Hong Kong.

10.1021/jp056548f CCC: $33.50
Published on Web 04/18/2006

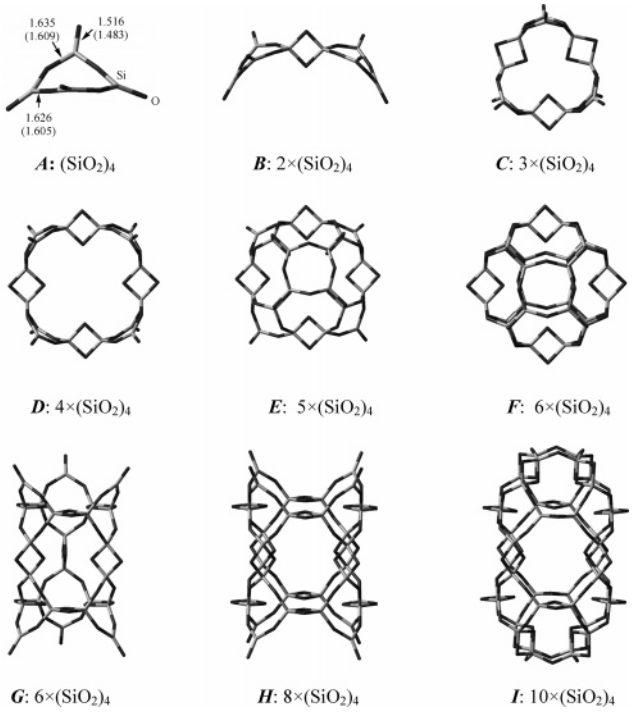

Figure 1. Silica nanostructures from the 4MR precursors, optimized at the B3LYP/6-31G(d) level of theory: (**A**) 4MR monomer with optimized Si−O bond lengths (Å) (values in parentheses are the results given by Xu et al. at the HF/6-31G(d) level, ref 34), (**B**) dimer fragment, (**C**) trimer ring, (**D**) tetramer ring, (**E**) pentamer semicage, (**F**) hexamer cage, (**G**) hexamer nanotube, (**H**) octamer nanotube, and (**I**) capped decamer nanotube. Gray sticks depart from Si atoms, and black sticks depart from O atoms.

In the present work, we describe discrete silica nanofullerenes and nanotubes formed from 4MR units, and study their geometrical, energetic, and electronic properties using high-level density functional calculations. We consider 4MRs as important building blocks of silica nanostructures based on the following background information: (i) 4MRs are present in almost 90% of all zeolite frameworks in various denser crystalline forms of silica and also within amorphous glassy silica,[35] and even are more frequent in nanometer-sized amorphous silica than in the bulk one;[36−38] (ii) as will be seen in the following section, isolated 4MRs are chemically reactive and likely coalesce into larger clusters; (iii) it is still not very clear how some of the fully coordinated silica nanostructures[21] proposed earlier are formed from certain easily identifiable building blocks, such as by either coalescence or hybridization between the small-membered rings, although Bromley has proposed a method of constructing fully coordinated silica structures by drawing a topology correspondence between hybridized carbon centers and silicon centers.[21]

We have performed systematic studies for the properties of 4MR-based silica structures, including their geometric and electronic structures, energetic and thermal stabilities, and chemical reactivities, using high-level density functional calculations. All results will be evaluated against the corresponding structural models proposed earlier.

2. Models and Calculations

Figure 1 shows the representative geometries of the silica clusters based on the precursor of 4MR, denoted as **A**−**I** in increasing order of cluster sizes, respectively. **A** is a basic unit of 4MR fragments, $(SiO_2)_4$, called the monomer, possessing four reactive NBO defect sites which promote the coalescence between small fragments. **B** denotes the dimer, $2(SiO_2)_4$, resulting from the interlinkage between two defect Si−O groups from each of two discrete 4MRs. In this structure, a 2MR is naturally formed between two 4MRs, which retains a perpendicular orientation to two directly adjacent 4MRs. This growth principle continues as the clusters further grow. **C** and **D**, two closed molecular rings, are the trimer and tetramer, respectively. **E** and **F** are the pentamer and hexamer, and the former is a semicage structure and the latter a fully coordinated cage. **G** is another configuration of the hexamer, a tubular structure, and **H** is the octamer, similar to **G** in geometry but with a larger diameter. The last one, **I**, is the decamer, a capped tube (or referred as an elongated cage), similar to a capped carbon nanotube.

The Gaussian 98 package[39] was used, and calculations were carried out at the B3LYP/6-31G(d) level of theory. To obtain the local-minimum structures unbiasedly, first, full geometry optimization calculations without any symmetry constraints were undertaken at the B3LYP/6-31G(d) level. Second, the initial structures were optimized again with keeping the point-group symmetry of the clusters. Once the optimized structures were obtained from both approaches, the harmonic vibrational frequencies were computed at the same level of theory to examine whether the optimized structures are the real minima of potential energy surfaces.

The relative energetic stability of the clusters was evaluated by calculating their binding energies (E_b), defined as the difference between the total energy of a cluster and the energy of the corresponding isolated SiO_2 molecules, as given by eq 1, where $E(SiO_2)$ and $E[(SiO_2)_n]$ are the energies of monomer

$$E_b = -\{E[(SiO_2)_n] - nE(SiO_2)\}/n \quad (1)$$

SiO_2 and its cluster $(SiO_2)_n$. The structural stability was tested by performing molecular dynamics simulations using the SIESTA 1.3 code[40] using the Perdew−Burke−Ernzerhof generalized gradient approximation (GGA) functional[41] with the double-ζ plus polarization orbital (DZP). The simulation time step was chosen to be 1 fs, and the relaxation steps were set to 1000. Atomic forces were calculated using the Hellmann−Feymann theorem; Newton's equations were integrated by means of Verlet's algorithm.

3. Results and Discussion

3.1. Geometrical Structure of the 4MR Monomer of Silica. As mentioned above, rhombic 2MR chains are the most stable structures for $n \leq 5$. This large stability is related to the small ratios of the NBO atoms. However, it should be noted that the suitability of a cluster/molecule to act as a material building block is not primarily/uniquely determined by its energy.[22] For example, in plasma experiments,[42] ground-state clusters are not necessarily formed, but metastable clusters normally occur. In view of the all-pervading occurrence of 4MRs in bulk and nanoscaled silica materials, they should be considered as the appropriate precursors or material building blocks for forming silica nanostructures, although they have been identically determined to be energetically less stable (by 2.57 eV from the present B3LYP/6-31G(d) calculations) than the corresponding ground-state structure.[15,16,32,33]

Our optimizations showed that the most stable configuration of the 4MR monomer is not the planar D_{4h} structure discovered by Harkless[32] and Nayak,[15] but rather a nonplanar structure with D_2 symmetry, as shown by **A** in Figure 1. This result agrees with that found by Xu et al.[33] at the HF/6-31G(d) level; however,

TABLE 1: Energy Change for Forming the 4MR-Based Silica Nanostructures

description	coalescence reaction	released energy (eV)
formation of the dimer	$2\mathbf{A} \rightarrow \mathbf{B}$	5.25
formation of the trimer ring	$\mathbf{A} + \mathbf{B} \rightarrow \mathbf{C}$	9.91
formation of the tetramer ring	$2\mathbf{B} \rightarrow \mathbf{D}$	10.35
formation of the semicage	$\mathbf{A} + \mathbf{D} \rightarrow \mathbf{E}$	18.54
formation of the cage	$\mathbf{A} + \mathbf{E} \rightarrow \mathbf{F}$	17.76
formation of the hexamer tube	$2\mathbf{C} \rightarrow \mathbf{G}$	15.40
formation of the octamer tube	$2\mathbf{D} \rightarrow \mathbf{H}$	20.60
capping of the octamer tube	$2\mathbf{A} + \mathbf{H} \rightarrow \mathbf{I}$	36.41

the Si−O bond length obtained earlier is slightly smaller than the present results since the electronic correlation effect was not taken into account enough. This 4MR configuration possesses four polar Si═O terminations, where the frontier HOMO and LUMO are located around these accessible terminating centers, thus facilitating orbital overlap and hence the coalescence between 4MR fragments.

3.2. Silica Nanostructures from 4MR Precursors. From metastable 4MRs with high growth reactivity, a series of tailored silica nanoarchitecures can be produced via coalescence between the precursors. Figure 1 shows the optimized geometries of the silica nanostructures, ranging in size from the dimer to the decamer, grown according to the desired growth principle. The energy changes in the growth of silica clusters is shown in Table 1.

For the dimer **B**, our calculations produce a stable C_{2v} structure with a naturally curved configuration, where two Si−O groups from each of the two 4MRs incorporate into a 2MR to form a symmetric double oxygen bridge between the two silicon atoms. This coalescence, a barrierless reaction, yields an association energy of 5.25 eV, as seen from Table 1, indicating that it is energetically very favorable. The highly exothermic property of this reaction is attributed to the effective reduction of NBO atoms, although the formation of a strained 2MR between two 4MRs plays an adverse role in stabilizing the cluster.

The coalescence continues as the silica cluster grows. A closed molecular ring (wheel) can be formed for the trimer **C** ($n = 12$) and tetramer **D** ($n = 16$). The former arises from the direct association between the monomer and dimer to release an energy of 9.91 eV, and the latter is a product resulting from the association between two dimers to release an energy of 10.35 eV. These exothermal association reactions indicate that the stabilization from the reduction of NBO atoms greatly exceeds the destabilization due to the strains of the ring and constituent 2MRs. These two rings contain three and four 2MRs, and are found having D_{3h} and D_{4h} symmetries, respectively. They can also be regarded as 2MR and 4MR uniformly hybrid structures. Unlike the 2MR molecular rings with fully coordinated structures proposed by Bromley,[17] our molecular ring possesses reactive NBO centers and can further grow. Here, we propose two possible growth models of silica nanostructures based on the tetramer molecular ring **D**: one is the silica fullerene cage, and the other is silica nanotubes. The parallelism between small stable fullerenes and nanotubes has been generally recognized since the discovery of C_{60} fullerene.[1] This parallelism is expected in silica systems in view of the porous structural characteristic of zeolites and successful synthesis of silica nanotubes.[7,8]

The semicage structure (Figure 1, structure **E**), a pentamer of $(SiO_2)_4$, can be formed by incorporating a 4MR monomer into the molecular ring **D**. The calculated association energy is 18.54 eV, much larger than that of the dimer. The reason is that eight NBO atoms can be turned into bridging oxygen atoms during this coalition, while only a pair of NBO atoms are associated in the formation of the dimer. Further, the silica fullerene cage (Figure 1, structure **F**) can be obtained via capping of the semicage structure by another 4MR. As shown in Figure 1, structure **F**, this fullerene cage contains six 4MRs and twelve 2MRs with high O_h symmetry. The same cage has been referred to in the context of testing the relative stability of the terminated and fully coordinated silica clusters.[19,22] However, its precursor was proposed from the sodalite cage $[Si_{24}O_{36}(OH)_{24}]$ rather than small silica fragments.[19] Instead, we constructed, here, this fully coordinated structure in an obvious route to its formation based on precursor (building block) 4MRs.

The other growth from the tetramer molecular ring (Figure 1, structure **D**) is the formation of a nanotube, as shown in Figure 1, structure **H**, which can be regarded as a simple association between the basic ring structures, releasing an energy of 20.60 eV. Our calculations obtained a uniformly hollow structure with a D_{4h} symmetry. During the growth of the tube, it is also possible for the tube to be closed in a cap, competing with its further growth. Figure 1, structure **I**, shows a capped nanotube (elongated cage) with a D_{4h} symmetry optimized at the same level, which can be regarded as the result obtained by incorporating two 4MR monomers into the ends of the tube. As listed in Table 1, this process is highly exothermal, releasing an energy of 36.41 eV. On the other hand, the capped nanotube can also be decapped and reconverted to a growing open-end structure, continuing the growth of the tubular structure. The optimized results show that the so-constructed silica nanotubes contain naturally open ends, which are necessary for the continuous growth of nanotubes. This case is very different from that of the previous 6MR nanotube reported by de Leeuw et al.[23] and Bromely,[21] where the initially designed active sites (dangling bonds) on both ends of the tube naturally form either three aligned or antialigned 2MRs after relaxation, resulting in a fully coordinated silica structure and hence the loss of the growth reactivity of the tube.

Similarly, a family of silica nanotubes can be obtained on the basis of the same growth principle. Figure 1, structure **G**, shows a so-constructed thin tube, which can be regarded as a product of the coalescence between two trimer molecular rings (Figure 1, structure **C**) to release an energy of 15.40 eV. Other tubes in this category are not shown for simplification.

3.3. Energetic and Structural Stabilities of the Silica Nanostructures. To reveal the relative stabilities of these new tailed nanoarchitecures, we calculated the variation of their binding energies with cluster size, and the relevant results are shown in Figure 2, curve a. Those of other types of silica clusters proposed earlier, including 2MR chains (curve b) and rings (curve c), 3MR-based structures (curve d), and 2MR−3MR hybrid structures (curve e), are also given for the sake of comparison. In line with previous results, we found that the isolated 4MR monomer is much higher in E_b than the corresponding 2MR chain, and also than the 2MR−3MR hybrid branch, mainly due to its larger number of NBO atoms. This unfavorable trend continues for the dimer, $2(SiO_2)_4$. With increasing cluster size, however, the tetramer, $4(SiO_2)_4$, has shown its slightly energetic predominance over the corresponding curved 3MR chains, although it is still very unfavorable compared to the other three structures. With further coalescence between the monomers, the stabilization rate of the new clusters becomes so large that it exceeds those of all four other types of silica clusters until $n = 24$. Note that there are two datum points for $n = 24$ (Figure 2), noted as "1" and "2", which correspond to the hexamer cage (Figure 1, structure **F**) and tube (Figure 1,

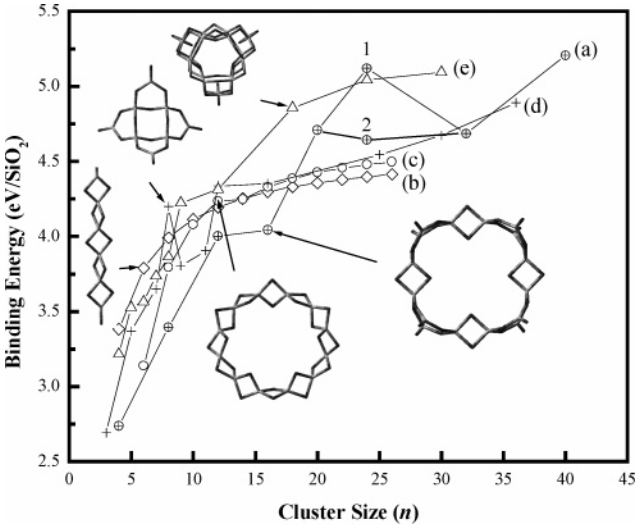

Figure 2. Variation of the binding energy (E_b) of the silica clusters as a function of the cluster size *n*, calculated at the B3LYP/6-31G(d) level for (a) the proposed 4MR-based structures, (b) 2MR chains, (c) 2MR rings, (d) pure 3MR structures, and (e) 2MR−3MR hybrid structures.

structure **G**), respectively. As shown by curve a, the former is a local minimum, indicating its high stability. In the present calculations, the cage was found to be 0.476 eV more stable in E_b than the hexamer tube, and also more favorable by 0.077 eV than the 2MR−3MR hybrid cage proposed earlier by us.[30] The octamer tube ($n = 32$) has an E_b value similar to that of the hexamer tube ($n = 24$), although its size is much larger than that of the latter. The reason is that these two tubes have the same ratio of the number of NBO atoms to *n*. As mentioned above, the formation of these metastable tubes can be envisaged by linking the rings, a thermodynamically downhill process, despite the less favorable E_b values compared to those of the fully coordinated structures. The formed tube can either continuously keep growing or be closed into the capped tube, which prevents further growth of the tube. The E_b of the capped tube for $n = 40$ was found to be comparable to that of the cage (5.206 eV vs 5.119 eV).

From these results, it is clear that these new clusters, based on 4MR precursors (in other words, referred to as 2MR−4MR hybrid clusters), become energetically more favorable than the 2MR chains and rings, and comparable to the other two types of clusters for the larger clusters; in particular, the cage for $n = 24$ was found much more stable than all previous types of silica clusters. In view of its anomalously high stability, we can regard this cage as a so-called "magic cluster", like a C_{60} fullerene cage. It should be able to be produced in cluster beams by favoring low-energy silica clusters.[13]

Further, we tested the structural stability of these desired nanostructures. We performed DFT molecular dynamics simulations by using SIESTA at several temperatures, i.e., 500, 1000, 1500, 2000, and 3000 K. We found that all these structures retain their initial connectivity throughout the whole simulation even at 3000 K, which is far higher than the synthesis conditions envisaged (∼1000 K). This fact indicates that the desired silica nanostructures are extremely thermally stable, and very resistant to collapse or rupture.

3.4. Electronic Properties of the Desired Silica Nanostructures. To reveal the electronic properties and the chemical reactivities of these new clusters, we calculated their HOMO and LUMO gaps and compared relevant results to those of the other types of silica clusters. As seen from curve a of Figure 3, the gaps of the cage (data point 1 in Figure 3) and the capped tube (7.19 and 7.25 eV, respectively) are remarkably higher than those of the other cluster fragments with NBO defects, indicating their high stabilities again. Further, we found that the HOMO state of the cage has a significant magnitude around the inner periphery of the cage (Figure 4a), located at the oxygen atoms, while the LUMO state mainly distributes around the outer periphery of the cage (Figure 4b), located at the silicon atoms. These characteristic electronic properties may find applications in nanotechnology, such as acting as new miniature chemical sensors to detect low concentrations of toxic gas molecules.

It is also seen from Figure 3 that the gaps of new clusters (except for the cage and capped tube) are comparable with those of 3MR clusters, and relatively smaller than those of the three other types of clusters, indicating their higher reactivities and growth activity, hence making them easily coalesced with each other into larger clusters. For instance, as seen from Figure 3, the gap of the hexamer tube (data point 2), 5.95 eV, is much smaller than that of the corresponding cage, 7.19 eV. Thus, these clusters would be expected to have a higher concentration in the medium and larger clusters, such as those larger than 20 atoms, and are expected to controllably grow into tailed silica nanoarchitectures.

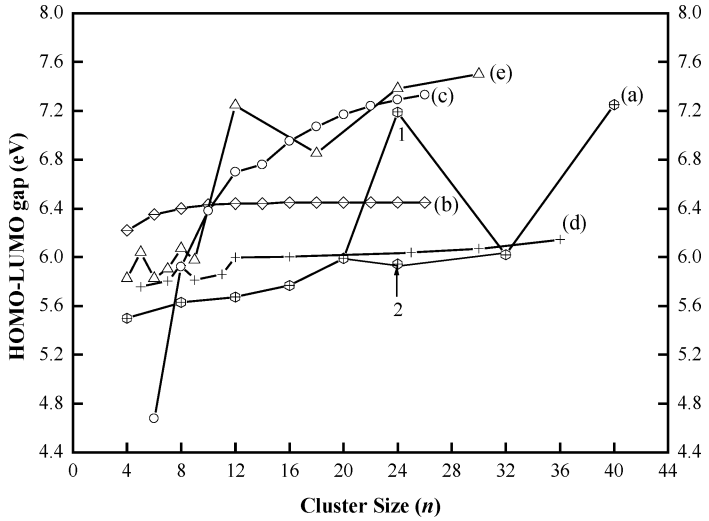

Figure 3. HOMO−LUMO gap versus the cluster size for (a) 2MR−4MR hybrid structures, (b) 2MR chains, (c) 2MR rings, (d) pure 3MR structures, and (e) 2MR−3MR hybrid structures.

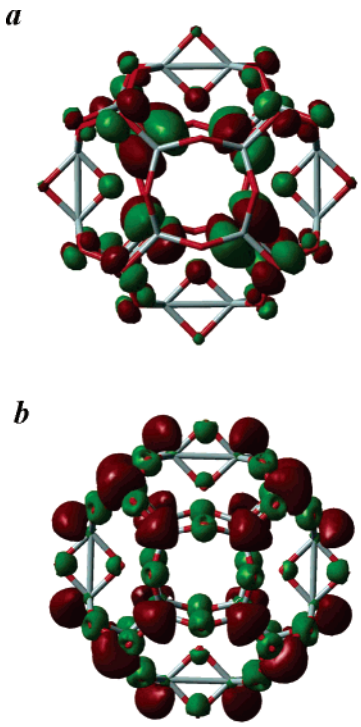

Figure 4. (a) HOMO and (b) LUMO orbitals with an isosurface value of 0.02 for the silica fullerene cage of $(SiO_2)_{24}$.

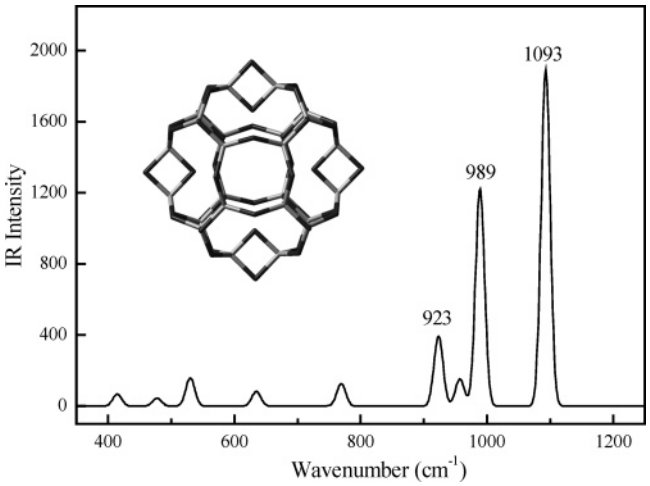

Figure 5. Calculated IR spectrum for the silica fullerene of $(SiO_2)_{24}$ at the B3LYP/6-31G(d) level of theory.

3.5. Vibrational Characteristic of the Discrete Silica Cage of $(SiO_2)_{24}$. Given the unusually high stability of the hexamer cage, we paid special attention to it. We calculated its vibrational property to provide the spectral signature for the experimental detection of the structure. The calculated result shows that all the frequencies are real, suggesting that this cage structure is stable dynamically. In its frequency spectrum (Figure 5), there are three prominent modes at 1093, 989, and 923 cm^{-1}. The mode with the maximum frequency and intensity is assigned to asymmetric stretching of the Si−O−Si bonds in the 4MR, while the other two with smaller frequencies and intensities correspond to symmetric stretching of the Si−O−Si bonds in the 2MRs. These spectroscopic fingerprints should provide good signatures for the experimental detection of this structure by infrared matrix isolation spectroscopy.

3.6. Relative Stability of the Hexamer Cage Compared to Its Other Fully Coordinated Isomers. To evaluate the relative stability of the present hexamer cage, we have also studied six other fully coordinated isomers of $(SiO_2)_{24}$, denoted as **I**−**VI**, as shown in Figure 6. Isomer **I** was constructed according to the connectivity of the C_{24} fullerene; i.e., all Si atoms are in the framework of the C_{24} fullerene and are connected by either single or double oxygen bridges.[21] Isomer **II** was regarded as one of the products of the thermolysis of the sodalite cage.[19] It has the same framework of Si atoms as the present hexamer cage shown in Figure 1, structure **G**, but a different arrangement of single and double oxygen bridges. These two cages are the most stable structures of $(SiO_2)_{24}$ found so far. Their energies are much closer to each other, and the former is only 0.03 eV more stable than the latter. Compared to these two most stable structures, our 4MR-based cage is only less favorable in energy by about 0.5 eV, indicating its comparable thermodynamic accessibility and hence the rationality of 4MRs acting as material building blocks of silica nanostructures. Isomers **III** and **V** are two tubular structures. The former is formed via coalescence between the spiro union 2MR rings,[23,32] and the latter consists of hybrid 2MRs and 3MRs.[31] They were found, from the present calculations, to be less stable in energy by 0.48 and 1.87 eV than our 4MR-based cage, respectively. The last two isomers, **V** and **VI**, are two molecular rings based on the spiro union 2MR,[29,32] which are less stable in energy by 5.20 and 13.39 eV than the hexamer cage, respectively. This can be mainly attributed to their larger ring strain.

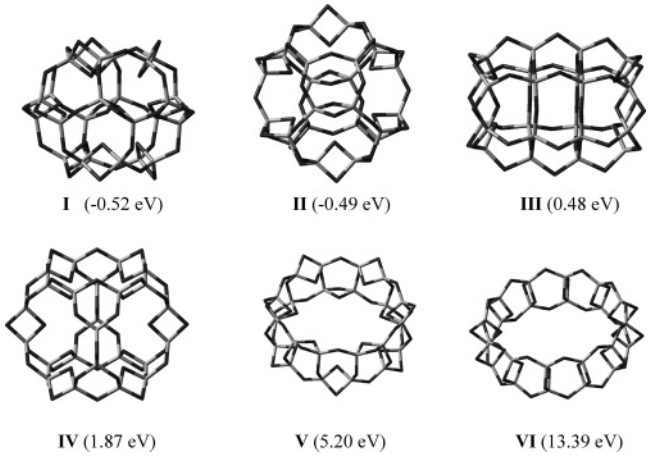

Figure 6. Six other isomers of the fully coordinated clusters of $(SiO_2)_{24}$ optimized at the B3LYP/6-31G(d) level. **I** has the framework of the C_{24} fullerene, **II** has the same framework of the present hexamer cage but with a different distribution of the double oxygen bridges, **III** is a 2MR−3MR hybrid structure,[30] **IV** is a short 6MR-based tube,[23] and **V** and **VI** are two molecular rings based on the spiro union 2MR.[29] Values in parentheses are energies relative to that of the hexamer cage shown in Figure 1, structure **E**.

In addition, we have also performed DFT calculations at the PBE1PBE/6-31G(d) level for isomers **I**−**III** of $(SiO_2)_{24}$ shown in Figure 6, to see whether the relative stability of silica clusters depends on the functional used. Our calculated results, however, show that there is no change of the order of the relative stability of these three isomers compared with that at the B3LYP/6-31G(d) level. This fact indicates that the global minima of silica clusters could be independent of the functional used, which is in contrast with that of silicon clusters.[43]

4. Conclusions

We have shown the formation mechanisms of silica fullerenes and nanotubes based on metastable 4MRs. By performing high-level DFT and MD calculations, we confirmed the desired structures are viable. The coalescences between the 4MR

fragments, resulting in the formation of silica nanocages and nanotubes, are thermodynamically accessible, and the so-formed cages and tubes are particularly resistant to collapse or rupture. The fabrication of these stable silica nanostructures is a challenge to the experimentalist, and if synthesized, they could find novel applications in nanotechnology.

Acknowledgment. The work described in this paper was supported by the National Science Foundation of China (Grant No. 20473047), the Major State Basic Research Development Programs (Grant No. 2004CB719902), and the Research Grants Council of the Hong Kong Special Administrative Region, China (Project No. CityU 103305). We thank the High Performance Computational Center of Shandong University for computer resources.

References and Notes

(1) Kroto, H. W.; Heath, J. R.; O'Brien, S. C.; Curl, R. F.; Smalley, R. E. *Nature (London)* **1985**, *318*, 162.
(2) Iijima, S. *Nature (London)* **1991**, *354*, 56.
(3) Lafargue, P. E.; Gaumet, J. J.; Muller, J. F.; Labrosse, A. *J. Mass Spectrom.* **1996**, *31*, 623.
(4) Schenkel, T.; Schlatholter, T.; Newman, M. W.; Machicoane, G. A.; McDonald, J. W.; Hamza, A. V. *J. Chem. Phys.* **2000**, *113*, 2419.
(5) Yu, D. P.; Hang, Q. L.; Ding, Y.; Zhang, H. Z.; Bai, Z. G.; Wang, J. J.; Zou, Y. H. *Appl. Phys. Lett.* **1998**, *73*, 3076.
(6) Hu, J. Q.; Jiang, Y.; Meng, X. M.; Lee, C. S.; Lee, S. T. *Chem. Phys. Lett.* **2003**, *367*, 339.
(7) Ji, Q.; Iwaura, R.; Kogiso, M.; Jung, J. H.; Yoshida, K.; Shimizu, T. *Chem. Mater.* **2004**, *16*, 250.
(8) Zygmunt, J.; Krumeich, F.; Nesper, R. *Adv. Mater.* **2003**, *15*, 1538.
(9) Cornelissen, J. J. L. M.; Conner, E. F.; Kim, H. C.; Lee, V. Y.; Magibitang, T.; Rice, P. M.; Volksen, W.; Sundberg, L. K.; Miller, R. D. *Chem. Commun.* **2003**, 1010.
(10) Sun, Q.; Kooyman, P. J.; Grossmann, J. G.; Bomans, P. H. H.; Frederik, P. M.; Magusin, P. C. M. M.; Beelen, T. P. M.; van Santen, R. A.; Sommerdijk N. A. J. M. *Adv. Mater.* **2003**, *15*, 1097.
(11) Muller, D. A.; Sorsch, T.; Moccio, S.; Baumann, F. H.; Evans-Lutterodt, K.; Timp, G. *Nature* **1999**, *399*, 758.
(12) Monnier, A.; Schuth, F.; Huo, Q.; Kumar, D.; Margolese, D.; Maxwell, R. S.; Stucky, G. D.; Krishnamurty, M.; Petroff, P.; Firouzi, A.; Janicke, M.; Chmelka B. F. *Science* **1993**, *261*, 1299.
(13) Wang, L. S.; Desai, S. R.; Wu, H.; Nicholas, J. B. *Z. Phys. D* **1997**, *40*, 36.
(14) Strobel, R.; Agashe, N.; Pratsinis, S. E.; Narayanan, T. *Nat. Mater.* **2004**, *3*, 370.
(15) Nayak, S. K.; Tao, B. K.; Khanna, N.; Jena, P. *J. Phys. Chem.* **1998**, *109*, 1245.
(16) Chu, T. S.; Zhang, R. Q.; Cheung, H. F. *J. Phys. Chem. B* **2001**, *105*, 1705.
(17) Bromley, S. T.; Zwijnenburg, M. A.; Maschmeyer, Th. *Phys. Rev. Lett.* **2003**, *90*, 035502.
(18) Bromley, S. T.; Zwijnenburg, M. A.; Maschmeyer, T. *Surf. Sci.* **2003**, *539*, L554.
(19) Zwijnenburg, M. A.; Bromley, S. T.; Flikkema, E.; Maschmeyer, T. *Chem. Phys. Lett.* **2004**, *385*, 389.
(20) Flikkema, E.; Bromley, S. T. *J. Phys. Chem. B* **2004**, *108*, 9638.
(21) Bromley, S. T. *Nano Lett.* **2004**, *4*, 1427.
(22) Bromley, S. T.; Zwijnenburg, M. A.; Flikkema, E.; Maschmeyer, Th. *Phys. Rev. Lett.* **2004**, *92*, 039602.
(23) de Leeuw, N. H.; Du, Z.; Li, J.; Yip, S.; Zhu, T. *Nano Lett.* **2003**, *3*, 1347.
(24) Sun, Q.; Wang, Q.; Kawazoe, Y.; Jena, P. *Nanotechnology* **2004**, *15*, 260.
(25) Lu, W. C.; Wang, C. Z.; Ho, K. M. *Chem. Phys. Lett.* **2003**, *378*, 225.
(26) Zhao, M. W.; Zhang, R. Q.; Lee, S. T. *Phys. Rev. Lett.* **2004**, *93*, 095503.
(27) Zhao, M. W.; Zhang, R. Q.; Lee, S. T. *Phys. Rev. B* **2004**, *69*, 153403.
(28) Zhao, M. W.; Zhang, R. Q.; Lee. S. T. *Phys. Rev. B* **2004**, *70*, 205404.
(29) Zhang, D. J.,; Zhang, R. Q. *Chem. Phys. Lett.* **2004**, *394*, 437.
(30) Zhang, D. J.,; Zhao, M. W.; Zhang, R. Q. *J. Phys. Chem. B* **2004**, *108*, 18451.
(31) D. J. Zhang, R. Q. Zhang, *J. Phys. Chem. B* **2006**, *110*, 1338.
(32) Harkless, J. A. W.,; Stillinger, D. K.; Stillinger, F. H. *J. Phys. Chem.* **1996**, *100*, 1098.
(33) Xu, C.; Wang, W.; Zhang, W.; Zhuang, J.; Liu, L.; Kong, Q.; Zhao, L.; Long, Y.; Fan, K.; Qian, S.; Li, Y. *J. Phys. Chem. A* **2000**, *104*, 9518.
(34) Lu, W. C.; Wang, C. Z.; Nguyen, V.; Schmidt, M. W.; Gordon, M. S.; Ho, K. M. *J. Phys. Chem. A* **2003**, *107*, 6936.
(35) Zwijnenburg, M. A.; Bromley, S. T.; van Alsenoy, C.; Maschmeyer, T. *J. Phys. Chem. A* **2002**, *106*, 12376.
(36) Umari, P.; Gonze, X.; Pasquarello, A. *Phys. Rev. Lett.* **2003**, *90*, 27401.
(37) Stolen, R. H.; Krause, J. T.; Kurkjian, C. R. *Discuss. Faraday Soc.* **1970**, *50*, 103.
(38) Galeener, F. L.; Lukovsky, G. *Phys. Rev. Lett.* **1976**, *37*, 1474.
(39) Frisch, M. J.; Trucks, G. W.; Schlegel, H. B.; Scuseria, G. E.; Robb, M. A.; Cheeseman, J. R.; Zakrzewski, V. G.; Montgomery, J. A., Jr.; Stratmann, R. E.; Burant, J. C.; Dapprich, S.; Millam, J. M.; Daniels, A. D.; Kudin, K. N.; Strain, M. C.; Farkas, O.; Tomasi, J.; Barone, V.; Cossi, M.; Cammi, R.; Mennucci, B.; Pomelli, C.; Adamo, C.; Clifford, S.; Ochterski, J.; Petersson, G. A.; Ayala, P. Y.; Cui, Q.; Morokuma, K.; Malick, D. K.; Rabuck, A. D.; Raghavachari, K.; Foresman, J. B.; Cioslowski, J.; Ortiz, J. V.; Baboul, A. G.; Stefanov, B. B.; Liu, G.; Liashenko, A.; Piskorz, P.; Komaromi, I.; Gomperts, R.; Martin, R. L.; Fox, D. J.; Keith, T.; Al-Laham, M. A.; Peng, C. Y.; Nanayakkara, A.; Gonzalez, C.; Challacombe, M.; Gill, P. M. W.; Johnson, B.; Chen, W.; Wong, M. W.; Andres, J. L.; Gonzalez, C.; Head-Gordon, M.; Replogle, E. S.; Pople, J. A. *Gaussian 98*, Revision A.7; Gaussian, Inc.: Pittsburgh, PA, 1998.
(40) Soler, J. M.; Artacho, E.; Gale, J. D.; García, A.; Junquera, J.; Ordejón, P.; Sánchez-Portal, D. *J. Phys.: Condens. Matter* **2002**, *14*, 2745.
(41) Perdew, J. P.; Burke, K.; Ernzerhof, M. *Phys. Rev. Lett.* **1996**, *77*, 3865.
(42) Kronik, L.; Fromherz, R.; Ko, E.; Gantefor, G.; Chelikowsky, J. R. *Nat. Mater.* **2002**, *1*, 49.
(43) Yoo, S.; Zeng, X. C. *J. Chem. Phys.* **2005**, *123*, 164303.